Equation-of-State Model for Temperature-Responsive Polymers with Tunable Response Onset

E. Manias* and Alexei M. Kisselev†

*Department of Materials Science and Engineering, 325-D Steidle Bldg, Pennsylvania State University, University Park, PA 16802, USA
†Department of Physics, Pennsylvania State University, University Park, PA 16802, USA

Abstract. [1] The phase behavior of aqueous solutions of temperature-responsive (ethylene oxide)/ethylene copolymers with tunable lower critical solution temperatures (LCST) is explored using an equation of state approach. The LCST in water of these polymers is tailored by their chemical composition, specifically by the balance of hydrophilic to hydrophobic groups in the polymer. The general formalism of the lattice-fluid with hydrogen-bonding theory, adjusted here to account for multiple types of hydrogen bonds, is employed, and the theoretical predictions are compared with experimental systems. The developed theoretical model is shown to be effective in describing the phase behavior of these systems, and the model parameters seem to be transferable between different homologous copolymer series.

Keywords: Equation-of-State Theory; Smart Polymers; Temperature-Responsive Polymers.
PACS: 82.60.Lf, 83.80.Rs, 82.35.Jk.

INTRODUCTION

Aqueous polymer solutions are abundant in nature and also important from a technological viewpoint [1], but, at the same time, represent systems whose theoretical description is rather challenging. These challenges arise from the fact that systems of molecules interacting with strong specific hydrogen-bonding interactions deviate remarkably from normal solution behavior [2, 3, 4, 5]. One such a deviation is the existence of a lower critical solution temperature (LCST), above which the polymer becomes insoluble in water, from which the temperature-sensitive solubility can be derived. There is a strong interest in designing polymer systems with a controlled solubility in water, since there is a variety of applications requiring smart/responsive materials for the potential use of such systems: sensors, actuators, cell patterning, and smart/triggered drug delivery, *etc*. Thus, an analytical model which would describe the LCST-type phase behavior of aqueous polymer solutions in a clear, concise and self-consistent manner and yet having a certain predictive power is very desirable.

Poly(ethylene oxide) (PEO) is probably one of the most investigated water-soluble polymers with an LCST , including considerable theoretical attention in recent years, particularly for PEO solution behavior [6, 7, 8]. Its LCST, associated with its ability to hydrogen bond to water, occurs at T$\geq$100 °C – *i.e.* above the boiling point of water at reasonable pressure– thus limiting its use for applications requiring a temperature-response. However, it has been shown that the LCST of water-soluble polymer can be tailored by controlling the relative amount of hydrophilic and hydrophobic segments in the polymer chain [9] –*e.g.* PEO's LCST can be decreased by *proper* addition of hydrophobic groups [10], as long as hydrophilic and hydrophobic segments are not lumped together in extended blocks (such a blockiness would facilitates micellar type of aggregates/collapse) [11, 12] rather than a 'normal' coil-to-globule transition [13]), which corresponds to a sharp LCST transition, determined by the hydrophilic/hydrophobic balance. This approach has been applied to a number of polymeric systems, including poly(N-isopropyl acrylamide) (PNIPAM) [14], poly(siloxyethylene glycol) [15], random copolymers of ethylene oxide and propylene oxide (EOPO) [16], as well as alternating segmented copolymers of ethylene oxide and ethylene (EO-EE) [17]. In this work, we will focus on this last type of oligo-ethylene-oxide/oligo-ethylene linear copolymers, which exhibit LCST phase behavior similar to that of pure poly(ethylene oxide) with a sharp LCST transition tailored at varied temperatures (from 7 to 80 °C) via the copolymer composition [17]. Specifically, focusing on these polymers, we describe their phase behavior by a well-established equation of state theoretical framework, the lattice-fluid with hydrogen-bonding [3, 18].

[1] CP963: Lecture Series on Computer and Computational Sciences

CP963, Vol 1, *Computational Methods in Science and Engineering, Theory and Computation: Old Problems and New Challenges*, edited by G. Maroulis and T. Simos

The specific goals of this study are (i) to apply the LFHB to the LCST phase behavior of (ethylene oxide)/ethylene copolymers, an application which necessitates a minor modification so as LFHB can address multiple types of hydrogen bonds; and (ii) to verify the assumption that the phase behavior of these systems is of the same nature as that of PEO, but with an LCST lowered in value by the hydrophobic character of the ethylene units.

THEORETICAL MODEL AND FRAMEWORK

From an Equation-of-State theoretical viewpoint, one can treat physical (van der Waals) interactions with the well-established Sanchez-Lacombe lattice-fluid (LF) model [2, 3], which is a compressible lattice theory (compressibility effects are also known to give rise to an LCST, in the general case of polymer solutions) and thus can overcome the limitations of incompressible classical Flory-Huggins theory that is unable to describe an LCST type of behavior [19]. In addition, combining the lattice-fluid approach with the chemical association approach [4] allows for the thermodynamic description of hydrogen-bonded polymer solutions. In lattice-fluid with hydrogen-bonding theory (LFHB) model, developed by Panayiotou and Sanchez [5], the physical contributions are treated with a lattice-fluid model and the chemical contributions are treated through an enumeration of pair interactions between various hydrogen-bonding donor and acceptor groups. The chemical (hydrogen-bonding) contributions of LFHB derived on the basis on the combinatorial expression for the number of ways of forming hydrogen bonds [20] extended so that it allows treat hydrogen-bonding in water [21]. Over the years the LFHB approach has been successfully tested in the extended range of external conditions on the phase behavior of a variety of fluid mixtures, including polymers and aqueous systems [18].

The basic approximation of the model is that physical (van der Waals) and chemical (hydrogen-bonding) forces are effectively decoupled, *i.e.*, the canonical partition function can be factored as

$$Q = Q_{LF} Q_{HB}, \tag{1}$$

so that one factor disregards the existence of hydrogen bonds and considers only physical intermolecular interactions, while the other factor takes into account only the hydrogen bonding. Physical interactions will be described in terms of lattice-fluid theory and chemical interactions will be applied only to proton-donor and acceptor groups forming hydrogen bonds.

We define our system to contain t types of molecules, with N_k molecules of k-th type at temperature T and external pressure P. Also, there are m types of proton-donor groups and n types of proton-acceptor groups, with ${d_i}^k$ being the number of donor groups of i-th type in each molecule of k-th type and, equivalently, ${a_j}^k$ being the number of acceptor groups of j-th type in each molecule of k-th type.

Lattice-Fluid

According to the lattice-fluid theory molecules are arranged on a quasi-lattice of N_r sites, N_0 of which are empty. Each molecule of k-th type is divided into r_k segments of close-packed volume v_k^* in the pure state and average (mean-field) interaction energy ε_k^*. The total number of lattice sites is then

$$N_r = rN + N_0 \quad \text{with} \quad r = \sum_{k=1}^{t} r_k x_k, \tag{2}$$

where rN is the total number of molecular segments in the system and x_k is the mole fraction of k-th component in the mixture ($x_k = N_k / \sum_{k=1}^{t} N_k$). The following combining and mixing rules are assumed

$$v^* = \sum_{k=1}^{t} \phi_k v_k^* \quad \text{and} \quad \varepsilon^* = \frac{1}{2} \left(\sum_{p=1}^{t} \phi_p s_p \right) \left(\sum_{k=1}^{t} \sum_{l=1}^{t} \theta_k \theta_l \varepsilon_{kl} \right), \tag{3}$$

where ϕ_k are the segment fractions (defined as $\phi_k = x_k r_k / r$) and θ_k are the surface fractions (defined as $\theta_k = \phi_k s_k / \sum_{l=1}^{t} \phi_l s_l$, where s_k is the average number of contacts per k-th segment, equivalent to a surface to volume ratio of that segment). A Berthelot-type combining rule is adopted for ε_{kl}

$$\varepsilon_{kl} = 2\xi_{kl} \left(\frac{\varepsilon_k^* \varepsilon_l^*}{s_k s_l} \right)^{1/2} \tag{4}$$

where ξ_{kl} is a dimensionless parameter, expected to have values close to unity. The total lattice-fluid volume of the system is given by

$$V_{LF} = N_r v^* = rNv^*\tilde{v}, \tag{5}$$

where the reduced volume ($\tilde{v} = 1/\tilde{\rho}$) is defined on the basis of a reduced density

$$\tilde{\rho} = \frac{rN}{N_r}. \tag{6}$$

Similarly, the total potential energy of the system, as derived in [3, 5] taking into account only nearest-neighbor interactions and ignoring interactions with empty sites, is given by

$$-E_{LF} = rN\tilde{\rho}\varepsilon^*. \tag{7}$$

On the basis of this definitions the canonical partition function of the physical interactions is given [5] by:

$$Q_{LF}(T, N_0, \{N_k\}) = (1-\tilde{\rho})^{-N_0}\tilde{\rho}^{-N}\prod_{k=1}^{t}\left(\frac{\omega_k}{\phi_k}\right)^{N_k}\exp\left[-\frac{E_{LF}}{RT}\right] \tag{8}$$

where ω_k is the number of configurations available to a r_k-mer in the close-packed pure state; ω_k is treated as a constant and will cancel out in all applications of interest here (this is not obvious in cases of PEO physisorption on solid surfaces, or in extreme, sub-R_g, confinements[22, 23, 24]).

Hydrogen-Bonding

The interaction energies due to hydrogen-bonding contribution are in excess of the physical interactions (which are accounted for by the lattice-fluid part of the partition function). For the hydrogen bond between a donor of the *i*-th type and an acceptor of the *j*-th type, we define ${E_{ij}}^0$ to be the favorable energy change upon hydrogen bonding, ${S_{ij}}^0$ the entropy loss associated with the (i, j) bond formation, and ${V_{ij}}^0$ the respective volume change. In the general case, there are N_{ij} bonds of the (i, j) type, thus the total hydrogen-bonding energy of the system is

$$E_{HB} = \sum_{i=1}^{m}\sum_{j=1}^{n} N_{ij}{E_{ij}}^0 \tag{9}$$

The number of ways of distributing the N_{ij} bonds among the functional groups of the system is given by the combinatorial expression corrected by the mean-filed probability of bond formation, as derived in [5]:

$$\Omega = \prod_{i=1}^{m}\frac{{N_d}^i!}{N_{i0}!}\prod_{j=1}^{n}\frac{{N_a}^j!}{N_{0j}!}\prod_{i}^{m}\prod_{j}^{n}\frac{{P_{ij}}^{N_{ij}}}{N_{ij}!} \tag{10}$$

where ${N_d}^i$ is the total number of donor groups of *i*-th type and ${N_a}^j$ is the total number of acceptor groups of *j*-th type

$${N_d}^i = \sum_{k=1}^{t} {d_i}^k N_k, \qquad {N_a}^j = \sum_{k=1}^{t} {a_j}^k N_k \tag{11}$$

leaving N_{i0} number of unbonded donors of *i*-th type and N_{0j} number of unbonded acceptors of *j*-th type

$$N_{i0} = {N_d}^i - \sum_{j=1}^{n} N_{ij}, \qquad N_{0j} = {N_a}^j - \sum_{i=1}^{m} N_{ij}, \tag{12}$$

and P_{ij} is the mean-field probability of (i, j) bond formation

$$P_{ij} = \frac{\tilde{\rho}}{rN}\exp\left[\frac{{S_{ij}}^0}{R}\right] \tag{13}$$

Following this formalism the canonical partition function for hydrogen bonding can by written as [5]

$$Q_{HB}(T,N_0,\{N_k\}) = \sum_{\{N_{ij}\}} \left(\frac{\tilde{\rho}}{rN}\right)^{\Sigma_{ij}N_{ij}} \prod_{i=1}^{m} \frac{{N_d}^i!}{N_{i0}!} \prod_{j=1}^{n} \frac{{N_a}^j!}{N_{0j}!} \times \\ \times \prod_{i}^{m}\prod_{j}^{n} \frac{1}{N_{ij}!} \exp\left[\frac{-N_{ij}(E_{ij}^0 - TS_{ij}{}^0)}{RT}\right] \tag{14}$$

Various hydrogen-bonding fractions are defined by

$$\nu_{ij} = \frac{N_{ij}}{rN}, \quad \nu_{i0} = \frac{N_{i0}}{rN}, \quad \nu_{0j} = \frac{N_{0j}}{rN}, \quad {\nu_d}^i = \frac{{N_d}^i}{rN}, \quad {\nu_a}^j = \frac{{N_a}^j}{rN} \tag{15}$$

Free energy and equations of state

The Gibbs free energy in a framework of the Lattice Fluid Theory with Hydrogen-Bonding (LFHB), developed by Panayiotou and Sanchez [5], consists of two terms: lattice-fluid and hydrogen-bonding

$$G = G_{LF} + G_{HB} \tag{16}$$

which follows immediately from the expression for the Gibbs partition function given by

$$\Psi(T,P,\{N_k\}) = \sum_{N_0=0}^{\infty} Q_{LF}(T,N_0,\{N_k\}) Q_{HB}(T,N_0,\{N_k\}) \exp[-\frac{PV}{RT}] \tag{17}$$

with $G = -kT\ln\Psi$ and V is the system volume

$$V = rN\tilde{v}v^* + \sum_{i=1}^{m}\sum_{j=1}^{n} N_{ij}{V_{ij}}^0 \tag{18}$$

While the reduced pressure ($\tilde{P}$) and reduced temperature ($\tilde{T}$) are:

$$\tilde{P} = P/P^* = Pv^*/\varepsilon^* \quad \text{and} \quad \tilde{T} = T/T^* = RT/\varepsilon^* \tag{19}$$

The lattice-fluid contribution can now be expressed by

$$\frac{G_{LF}}{k_BT} = rN\left\{-\frac{\tilde{\rho}}{\tilde{T}} + \frac{\tilde{P}\tilde{v}}{\tilde{T}} + (\tilde{v}-1)\ln(1-\tilde{\rho}) + \frac{1}{r}\ln\tilde{\rho} + \sum_{k=1}^{t}\frac{\phi_k}{r_k}\ln\frac{\phi_k}{\omega_k}\right\} \tag{20}$$

and the hydrogen-bonding contribution is given by

$$\frac{G_{HB}}{k_BT} = rN\left\{\sum_{i=1}^{m}\sum_{j=1}^{n}\nu_{ij} + \sum_{i=1}^{m}{\nu_d}^i\ln\frac{\nu_{i0}}{{\nu_d}^i} + \sum_{j=1}^{n}{\nu_a}^j\ln\frac{\nu_{0j}}{{\nu_a}^j}\right\} \tag{21}$$

The Gibbs partition function was evaluated in the usual way by using the maximum term approximation [25]. This is equivalent to using the generic term in (17) for the Gibbs free energy, (substituting the factorials with the Stirling approximation) and implying the minimization conditions with respect to $\tilde{v}$ and N_{ij}

$$\left(\frac{\partial G}{\partial\tilde{v}}\right)_{T,P,\{N_k\},\{N_{ij}\}} = 0 \quad \text{and} \quad \left(\frac{\partial G}{\partial N_{ij}}\right)_{T,P,\tilde{v},\{N_k\},\{N_{rs}\}} = 0 \tag{22}$$

The first condition of (22) yields the equation of state for the reduced density

$$\tilde{\rho}^2 + \tilde{P} + \tilde{T}\left[\ln(1-\tilde{\rho}) + \tilde{\rho}\left(1-\frac{1}{r}\right)\right] = 0 \tag{23}$$

where

$$\frac{1}{\tilde{r}} = \frac{1}{r} - \nu_H, \qquad \nu_H = \sum_{i=1}^{m}\sum_{j=1}^{n} \nu_{ij}. \tag{24}$$

The second condition in (22) yields a system of equations for the fractions of hydrogen bonds in the system

$$\frac{\nu_{ij}}{\nu_{i0}\nu_{0j}} = \tilde{\rho} \exp\left[\frac{-{G_{ij}}^0}{RT}\right] \tag{25}$$

where ${G_{ij}}^0 = {E_{ij}}^0 + P{V_{ij}}^0 - T{S_{ij}}^0$. The reduced density equation of state (23) and the H-bond fractions equations (25) are used together and can serve as a system of equations of state

$$\begin{cases} \tilde{\rho}^2 + \tilde{P} + \tilde{T}\left[\ln(1-\tilde{\rho}) + \tilde{\rho}\left(1 - \frac{1}{\tilde{r}}\right)\right] = 0 \\ \nu_{i0}\nu_{0j}\tilde{\rho} - \nu_{ij}\exp\left({G_{ij}}^0/RT\right) = 0 \end{cases} \tag{26}$$

Chemical potential of k-th component is obtained as follows

$$\mu_k = \left(\frac{\partial G_{LF}}{\partial N_k}\right)_{T,P,N_j,\tilde{\nu},\{N_{ij}\}} + \left(\frac{\partial G_{HB}}{\partial N_k}\right)_{T,P,N_j,\tilde{\nu},\{N_{ij}\}} = \mu_{k,LF} + \mu_{k,HB} \tag{27}$$

and is given by

$$\begin{aligned} \frac{\mu_k}{k_B T} &= \ln\phi_k + \left(1 - \frac{r_k}{r}\right)\phi_k + \\ &+ r_k\tilde{\rho}\left(\sum_{i<k}\theta_i\frac{s_k}{s_i}X_{ik} + \sum_{i>k}\theta_i X_{ki} - \sum_{i<j}\theta_i\theta_j\frac{s_k}{s_i}X_{ij}\right) + \\ &+ r_k\left(\frac{-\tilde{\rho} + \tilde{P}_k\tilde{\nu}}{\tilde{T}_k} + (\tilde{\nu}-1)\ln(1-\tilde{\rho}) + \frac{1}{r_k}\ln\frac{\tilde{\rho}}{\omega_k}\right) + \\ &+ r_k\sum_{i=1}^{m}\sum_{j=1}^{n}\nu_{ij} - \sum_{i=1}^{m} {d_i}^k \ln\frac{{\nu_d}^i}{\nu_{i0}} - \sum_{j=1}^{n} {a_j}^k \ln\frac{{\nu_a}^j}{\nu_{0j}}, \end{aligned} \tag{28}$$

where

$$X_{kl} = \left(\varepsilon_k^* + (s_k/s_l)\varepsilon_l^* - 2\xi_{kl}\sqrt{(s_k/s_l)\varepsilon_k^*\varepsilon_l^*}\right)/RT \tag{29}$$

is the reduced average interaction between k-mer and l-mer and $\tilde{P}_k = P/P_k^* = Pv_k^*/\varepsilon_k^*$ and $\tilde{T}_k = T/T_k^* = RT/\varepsilon_k^*$

Binary mixture

Focusing on the phase behavior of a polymer-solvent binary mixture (index 1 denotes solvent, and index 2 polymer) r becomes $r = r_1x_1 + r_2x_2$, and the mole fractions (x_i) are simply:

$$x_2 = N_2/(N_1+N_2), \quad x_1 = N_1/(N_1+N_2) = 1 - x_2 \tag{30}$$

and the corresponding segment fractions (ϕ_i)

$$\phi_2 = r_2x_2/r, \quad \phi_1 = r_1x_1/r = 1 - \phi_2 \tag{31}$$

and the surface fractions become

$$\theta_2 = \frac{\phi_2}{\phi_2 + \phi_1(s_1/s_2)}, \quad \theta_1 = \frac{\phi_1}{\phi_1 + \phi_2(s_2/s_1)} = 1 - \theta_2 \tag{32}$$

where s_1/s_2 is ratio of the surface area per unit characteristic volume for solvent and polymer and can be calculated/approximated by a hard-sphere model or via van der Waals radii. The mixing and combining rules simplify to

$$v^* = \phi_1 v_1^* + \phi_2 v_2^* \tag{33}$$

$$\varepsilon^* = \phi_1 \varepsilon_1^* + \phi_2 \varepsilon_2^* - \phi_1 \theta_2 X_{12}, \tag{34}$$

where

$$X_{12} = \left(\varepsilon_1^* + (s_1/s_2)\varepsilon_2^* - 2(s_1/s_2)^{1/2} \varepsilon_{12}^* \right) / RT \tag{35}$$

and

$$\varepsilon_{12}^* = \xi_{12} (\varepsilon_1^* \varepsilon_2^*)^{1/2} \tag{36}$$

The dimensionless parameter ξ_{12} is the only free parameter of the model, and is expected to have values close to unity.

In the binary case of the model, the phase behavior can be determined in terms of two independent variables –composition x_2 and temperature T– along with a number of parameters, including external pressure P. External pressure is always kept constant in our considerations, thus it is treated as a parameter rather than a variable. Other parameters of the model include, from the lattice-fluid part: average interaction energies ε_1^*, ε_2^*, close-packed volumes v_1^*, v_2^*, and numbers of segments r_1, r_2; and, from the hydrogen-bonding part, for each (i, j) bond type: favorable energy change ${E_{ij}}^0$, entropy loss ${S_{ij}}^0$, and volume change ${V_{ij}}^0$. All these parameters can be obtained from experimental PVT data, from mixing rules, and from hydrogen-bonding interactions data, all of which can be found in literature for a variety of components [25].

The coexistence curve (binodal) –depicting the composition of coexisting phases at different temperatures– is obtained by the typical thermodynamic stipulation that the chemical potential of both component is the same in all coexisting phases, i.e. at a given temperature T mole fraction points ${x_2}^A$ and ${x_2}^B$ belong to the binodal curve if the following condition is satisfied

$$\begin{cases} {\mu_1}^A - {\mu_1}^B = 0 \\ {\mu_2}^A - {\mu_2}^B = 0 \end{cases} \tag{37}$$

To find a pair of binodal points one needs to solve (37) and the system of equations of state (26) simultaneously. The corresponding spinodal curve, which separates the region of thermodynamic instability from the region of metastability and at a given temperature T, is determined by

$$\frac{\mathrm{d}\mu_2}{\mathrm{d}x_2} = 0 \tag{38}$$

Consequently, it is required to solve simultaneously (38) with the system of equations of state (26) and the system of first composition derivatives $\mathrm{d}/\mathrm{d}x_2$ of the equations of state. The extremum point of the spinodal curve, corresponding to the critical point of the system, is given by

$$\frac{\mathrm{d}^2\mu_2}{\mathrm{d}x_2^2} = 0 \tag{39}$$

Finding a critical point is equivalent to the simultaneous solution of (39) with the system of equations of state (26) along with first $\mathrm{d}/\mathrm{d}x_2$ and second $\mathrm{d}^2/\mathrm{d}x_2^2$ composition derivatives of the equations of state, which adds up to a rather large system of nonlinear equations. The system of this size and complexity cannot be solved analytically even in relatively simple cases, thus requiring a numerical approach to the finding of the solution. The explicit form of the equations for binodal, spinodal and critical point follow immediately from the expressions for the chemical potentials and the equations of state as presented in Results and Discussion, whereas the numerical solution procedure is outlined in the next section.

Numerical procedure

Experimental polymer/water phase diagrams were fitted with the present model using a nonlinear least-squares procedure. Naturally, the fitting process involved the finding of numerical solution of the system of equations (37) repeatedly for different values of parameter ξ_{12}. To facilitate the numerical procedure and to avoid the finding of the trivial solution, equations (37) were rewritten in the following equivalent form

$$\begin{cases} \left(1 - \dfrac{{\mu_1}^B}{{\mu_1}^A}\right) \dfrac{1}{{x_2}^A - {x_2}^B} = 0 \\ \left(1 - \dfrac{{\mu_2}^B}{{\mu_2}^A}\right) \dfrac{1}{{x_2}^A - {x_2}^B} = 0 \end{cases} \tag{40}$$

The system of binodal equations (40) and the equations of state (26) was solved numerically using the trust-region dogleg method [26]. It appears to be more logical to build a binodal curve by solving for ${x_2}^B$ and T for a series of ${x_2}^A$ values, instead of solving for ${x_2}^A$ and ${x_2}^B$ for every given temperature value. Due to the system complexity, the choice of initial approximation is crucial to the successful finding of the roots and has to be automated in order to be used in the fitting procedure. Fortunately, the system of the spinodal equations has a much better tolerance to the initial approximation, which allows to solve for a point on the spinodal curve, which, in turn, can be used as a good initial approximation for the solution of the critical point equations (taking into account the fact that the critical point is the extremum of the spinodal curve). Taking two points closely on opposite sides of the critical point provides a sufficiently good initial approximation for the system of the binodal equations. Naturally, after the first pair of binodal points is found, it is used as the initial approximation for the solution at the next value of ${x_2}^A$; granted sufficiently small step size, the described algorithm can be fully automated and can successfully construct a binodal which can fit the experimental phase diagram data.

RESULTS AND DISCUSSION

PEO/water model

Probably the most investigated polymer with an LCST in water solution is poly(ethylene oxide) (PEO). It has been established, both experimentally and theoretically, that the phase behavior of PEO in water is determined by the hydrogen bonding balance between water and PEO molecules. Let us first consider an application of LFHB theory to the case of water/PEO mixture. Each OH group acts as both a donor and an acceptor, thus a water molecule has ${d_1}^1 = 2$ donors and ${a_1}^1 = 2$ acceptors. Let us denote the number of –O– groups per PEO molecule with a, hence the PEO molecule has ${a_2}^2 = a$ acceptors, where a is the degree of polymerization of PEO. There will be two types of H-bonds in this system $(1,1)$ and $(1,2)$, water–water and water–polymer correspondingly. Chemical potential of the

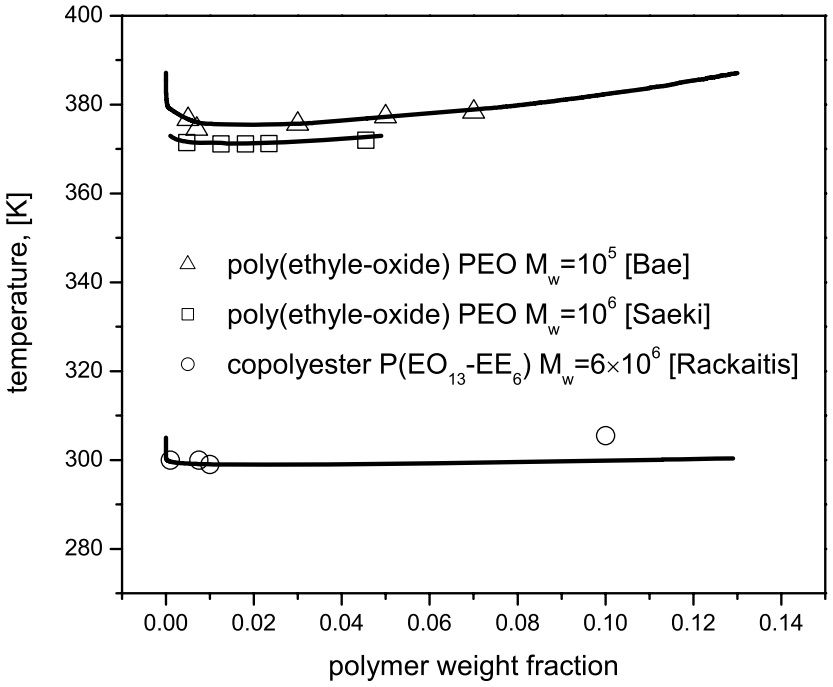

FIGURE 1. Experimental coexistence curves fitted with calculated binodals (solid line).

TABLE 1. Lattice-fluid and hydrogen-bonding parameters

Lattice-fluid			
	T^* K	P^* Pa	ρ^* kg/m^3
H_2O	518	$4.75\cdot10^8$	853
PEO	541	$6.05\cdot10^8$	1172
Hydrogen-bonding			
	E_{ij}^0 J/mol	${S_{ij}}^0$ J/mol·K	${V_{ij}}^0$ m^3/mol
–OH ··· –OH	$-1.55\cdot10^4$	-16.6	$-4.2\cdot10^{-6}$
–OH ··· –O–	$-1.42\cdot10^4$	-16.0	$-8.5\cdot10^{-7}$
–OH ··· C=O	$-1.60\cdot10^4$	-15.8	$-8.5\cdot10^{-7}$
N–H ··· –OH	$-1.25\cdot10^4$	-7.8	$-8.5\cdot10^{-7}$

polymer $\mu_2 = \mu_{2,LF} + \mu_{2,HB}$ and of water $\mu_1 = \mu_{1,LF} + \mu_{1,HB}$ can be obtained from (28), by rewriting for the binary case of two types of hydrogen bonds

$$\begin{aligned}
\frac{\mu_{2,LF}}{k_BT} &= \ln\phi_2 + \left(1-\frac{r_2}{r_1}\right)\phi_1 + r_2\tilde{\rho}\,\theta_1^2 X_{21} + r_2\left\{\frac{\tilde{P}_2\tilde{v}-\tilde{\rho}}{\tilde{T}_2} + (\tilde{v}-1)\ln(1-\tilde{\rho}) + \frac{1}{r_2}\ln\frac{\tilde{\rho}}{\omega_2}\right\} \\
\frac{\mu_{2,HB}}{k_BT} &= r_2(\nu_{11}+\nu_{12}) + {a_2}^2\ln\left(1-\frac{r\nu_{12}}{{a_2}^2x_2}\right)
\end{aligned} \tag{41}$$

$$\begin{aligned}
\frac{\mu_{1,LF}}{k_BT} &= \ln\phi_1 + \left(1-\frac{r_1}{r_2}\right)\phi_2 + r_1\tilde{\rho}\,\theta_2^2 X_{12} + r_1\left\{\frac{\tilde{P}_1\tilde{v}-\tilde{\rho}}{\tilde{T}_1} + (\tilde{v}-1)\ln(1-\tilde{\rho}) + \frac{1}{r_1}\ln\frac{\tilde{\rho}}{\omega_1}\right\} \\
\frac{\mu_{1,HB}}{k_BT} &= r_1(\nu_{11}+\nu_{12}) + {d_1}^1\ln\left(1-\frac{r(\nu_{11}+\nu_{12})}{{d_1}^1x_1}\right) + {a_1}^1\ln\left(1-\frac{r\nu_{11}}{{a_1}^1x_1}\right)
\end{aligned} \tag{42}$$

There will be three equations of state - one for the reduced density and one for the H-bond fraction of each type ν_{11} and ν_{12} as follows from (26)

$$\begin{cases}
\tilde{\rho}^2 + \tilde{P} + \tilde{T}\left(\ln(1-\tilde{\rho}) + \tilde{\rho}\left(1-\dfrac{1}{\bar{r}}\right)\right) = 0 \\
\mathscr{D}_1\mathscr{A}_1 - r\nu_{11}A_{11} = 0 \\
\mathscr{D}_1\mathscr{A}_2 - r\nu_{12}A_{12} = 0
\end{cases} \tag{43}$$

where

$$\begin{aligned}
\mathscr{D}_1 &= {d_1}^1x_1 - r(\nu_{11}+\nu_{12}) & A_{11} &= r\tilde{v}\exp\left({G_{11}}^0/RT\right) \\
\mathscr{A}_1 &= {a_1}^1x_1 - r\nu_{11} & A_{12} &= r\tilde{v}\exp\left({G_{12}}^0/RT\right) \\
\mathscr{A}_2 &= {a_2}^2x_2 - r\nu_{12}
\end{aligned} \tag{44}$$

Lattice-fluid and hydrogen-bonding parameters of the model, shown in Table 1, are obtained from the literature [5, 27, 28]. Tabulated data can be translated into the terms of LFHB model via obvious relationships

$$\varepsilon_k^* = RT_k^* \quad v_k^* = \varepsilon_k^*/P_k^* \quad r_k = M_{wk}/\rho_k^* v_k^* \tag{45}$$

where M_{wk} is the molecular weight of k-th component. The ratio of surface areas per unit characteristic volume for water and ethylene oxide can be calculated based on hard-sphere model to be $(s_1/s_2)^{EO} = 1.3424$. Dimensionless variable ξ_{12} is treated as a free parameter of the model.

Finding the pair of binodal points at given temperature T involves solving the system of 8 nonlinear equations, finding a concentration and a temperature of a spinodal point is equivalent to solving the system of 7 equations, and the critical point can be found as a solution to the system of 11 equations, solved numerically as described in the Numerical procedure section.

At the limit of high molecular weights the phase behavior of polymers becomes almost molecular weight independent, which allows us in the first approximation to disregard the effects of the molecular weight, i.e. keep M_w in all of our calculations in this section constant and equal to $6 \cdot 10^5$, the approximate molecular weight of $m = 13, n = 6$ ester copolymer [17]. Following this approach, the phase diagram of $M_w = 10^5$ PEO [29] was fitted with the calculated PEO binodal using the numerical procedure described in the Appendix, yielding a value for the dimensionless interaction parameter ${\xi_{12}}^{EO} = 1.0472$, the experimental and the calculated phase diagrams are shown in Figure 1. This value of ${\xi_{12}}^{EO}$ was used in later calculations of the phase diagrams of our "polyester" and "polyamide" ethylene oxide copolymers without any further change.

P(EO-EE)/water model

The polymers of interest are based on a linear alternating sequence of oligo(m)-EO and oligo(n)-EE [17] with the aim of tailoring polymer LCST by controlling the hydrophilic/hydrophobic balance (m/n). These copolymers exhibit phase behavior that appears similar to that of PEO, but have an LCST at substantially lower temperatures. One of the goals of this study is to see whether the LFHB model of PEO as presented above can be extended to describe the phase behavior of the $[(EO)_m - (EE)_n]$ copolymer, which would imply that the copolymer phase behavior can be considered similar in nature as the aqueous phase behavior of PEO only temperature-shifted by the hydrophobic EE group contributions. This can be done by introducing the following simple combination rule (the weighted average)

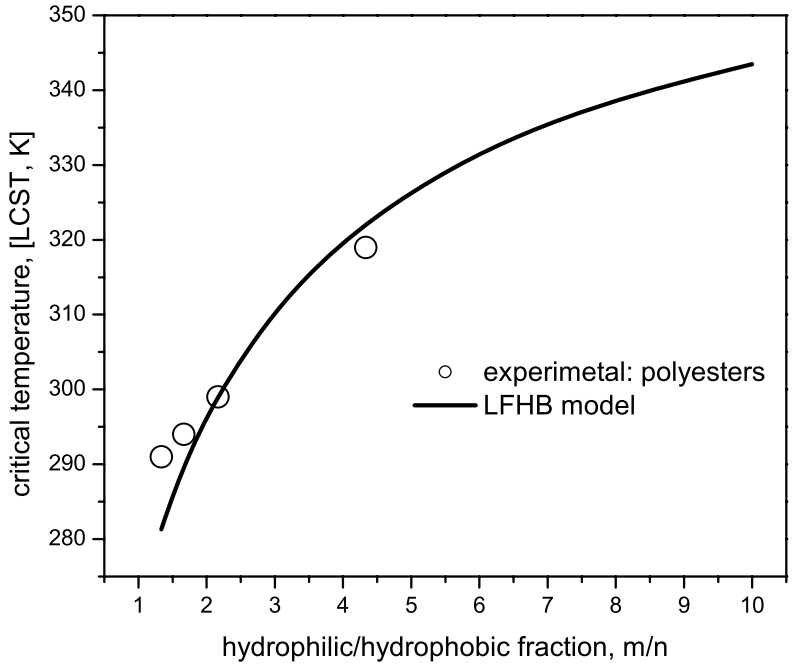

FIGURE 2. LCST dependence on hydrophilic/hydrophobic balance m/n for the general case of $[(EO)_m - (EE)_n]$ copolymer as described in section P(EO-EE)/water model.

for the EO and EE dimensionless parameters

$$\xi_{12} = \frac{m}{m+n}{\xi_{12}}^{EO} + \frac{n}{m+n}{\xi_{12}}^{EE}$$
$$\frac{s_1}{s_2} = \frac{m}{m+n}\left(\frac{s_1}{s_2}\right)^{EO} + \frac{n}{m+n}\left(\frac{s_1}{s_2}\right)^{EE} \tag{46}$$

The ratio of surface areas per unit characteristic volume for water and ethylene can be calculated based on the hard-sphere model $(s_1/s_2)^{EE} = 1.3266$, and ${\xi_{12}}^{EE}$ can be obtained from the best fit of the experimental phase diagram of one of the P(EO-EE) copolymers. Replacement of EO segments with EE segments decreases the number of hydrogen bonding sites per polymer molecule, effectively reducing the hydrogen bonding interactions, which is expected to result in lowering of the LCST. The model produces satisfactory results in terms of describing the phase behavior of the series of copolymers as a function of hydrophilic/hydrophobic balance m/n with no further modifications (Figure 2), simply by scaling the number of hydrogen bonding sites per polymer molecule to be equal to ${a_2}^2 = ({a_2}^2)^{PEO} \cdot m/(m+n)$, where $({a_2}^2)^{PEO} = M_{\mathrm{w}}^{poly}/M_{\mathrm{w}}^{EO}$.

The application of the model to P(EO-EE) was tested in the most simple case, which ignores the presence of the linkage groups and accounts for the difference between PEO and P(EO-EE) by using the combination rule for dimensionless parameters and by appropriate rescaling of the number of the polymer hydrogen bonding sites as described above. The dimensionless interaction parameter ${\xi_{12}}^{EE} = 1.0860$ was obtained from the fit of the experimental coexistence curve of an $m = 13$, $n = 6$ ester copolymer [17] with the LFHB binodal. This value of ${\xi_{12}}^{EE}$ arguably contains implicit contributions from the ester groups that link the EE and EO sequences. Despite the crudeness of this first approximation, LFHB can capture the trends of the experimental data for the dependence of the calculated LCSTs on the hydrophilic/hydrophobic ratio m/n for these ester copolymers. The phase behavior of another homologous series of EO/EE copolymers containing amide groups can be described in the same manner, but will obviously require obtaining different value for the ξ_{12}^{EE} parameter (since now this parameter will contain implicitly contributions from the amide linkage groups). Given that the differences in phase behavior of these homologous polyester and polyamide copolymers should be explained by accounting for the differences between the respective linkage groups, it is more desirable to extend the model to include the linkage groups explicitly by introducing a more rigorous H-bonding counting scheme, and fix the ξ_{12}^{EE} parameter to be the same across all EE-containing copolymers with different linkage chemistries.

Polyester EO-EE copolymers

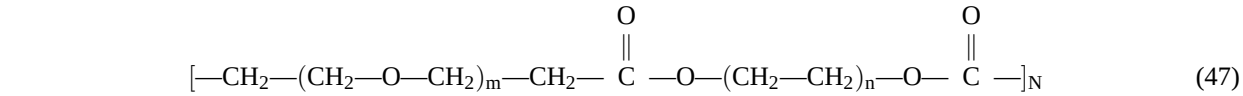

$$[\text{—CH}_2\text{—(CH}_2\text{—O—CH}_2)_{\mathrm{m}}\text{—CH}_2\text{—}\ \underset{\underset{\|}{\mathrm{O}}}{\mathrm{C}}\ \text{—O—(CH}_2\text{—CH}_2)_{\mathrm{n}}\text{—O—}\ \underset{\underset{\|}{\mathrm{O}}}{\mathrm{C}}\ \text{—}]_{\mathrm{N}} \tag{47}$$

The ester oxygen (C=O) in the polyester copolymers (47) introduces an additional type of acceptor to the model. Now there are three types of H-bonds: $(1,1)$, $(1,2)$, $(1,3)$ - water–water, water–polymer(ether oxygen, –O–), water–polymer(ester oxygen, C=O). Each water molecule has ${d_1}^1 = 2$ donors and ${a_1}^1 = 2$ acceptors of the first type, each P(EO-EE) molecule has ${a_2}^2 = m \cdot \mathrm{N}$ acceptors of the second type, equal to the number of EO segments, and ${a_3}^2 = 2 \cdot \mathrm{N}$ acceptors of the third type, equal to the number of C=O groups. We can assume that the van der Waals contribution from the C=O groups to the lattice-fluid part of the model will be contained in the contribution from EE segments and thus can be accounted for by the binodal fitting through the combination rule (46). This leaves the lattice-fluid part unchanged, except for the modified value of the dimensionless parameters ξ_{12}^{EE}, but it introduces one additional term to the hydrogen bonding part of the chemical potential

$$\frac{\mu_{2,HB}}{k_B T} = r_2(\nu_{11}+\nu_{12}+\nu_{13}) + {a_2}^2 \ln\left(1 - \frac{r\nu_{12}}{{a_2}^2 x_2}\right) + {a_3}^2 \ln\left(1 - \frac{r\nu_{13}}{{a_3}^2 x_2}\right) \tag{48}$$

$$\frac{\mu_{1,HB}}{k_B T} = r_1(\nu_{11}+\nu_{12}+\nu_{13}) + {d_1}^1 \ln\left(1 - \frac{r(\nu_{11}+\nu_{12}+\nu_{13})}{{d_1}^1 x_1}\right) + {a_1}^1 \ln\left(1 - \frac{r\nu_{11}}{{a_1}^1 x_1}\right) \tag{49}$$

Introduction of the third type of hydrogen bond adds another equation to the system of the equations of state, the reduced density equation remains unchanged, and the hydrogen-bonding part has the following form

$$\begin{cases} \mathscr{D}_1\mathscr{A}_1 - r\nu_{11}A_{11} = 0 \\ \mathscr{D}_1\mathscr{A}_2 - r\nu_{12}A_{12} = 0 \\ \mathscr{D}_1\mathscr{A}_3 - r\nu_{13}A_{13} = 0 \end{cases} \quad \text{where} \quad \begin{array}{l} \mathscr{D}_1 = {d_1}^1 x_1 - r(\nu_{11} + \nu_{12} + \nu_{13}) \\ \mathscr{A}_1 = {a_1}^1 x_1 - r\nu_{11} \\ \mathscr{A}_2 = {a_2}^2 x_2 - r\nu_{12} \\ \mathscr{A}_3 = {a_3}^2 x_2 - r\nu_{13} \end{array} \quad \begin{array}{l} A_{11} = r\tilde{\nu}\exp\left({G_{11}}^0/RT\right) \\ A_{12} = r\tilde{\nu}\exp\left({G_{12}}^0/RT\right) \\ A_{13} = r\tilde{\nu}\exp\left({G_{13}}^0/RT\right) \end{array} \tag{50}$$

which results in finding the critical point being equivalent to a solution to the system of 14 equations.

Lattice-fluid and hydrogen-bonding parameters of the model from Table 1 can be used in the model with the equations (45) and (46). The ratio $(s_1/s_2)^{EE} = 1.3266$ was calculated based on hard-sphere model, and the dimensionless parameter ξ_{12}^{EE} can be obtained from fitting the experimental phase diagram of polyester; for example, ${\xi_{12}}^{EE} = 1.0537$ is obtained by fitting experimental phase diagram for $M_w = 6 \cdot 10^5$, $m = 13$, $n = 6$ polyester with the binodal calculated for the EO-EE copolymer with the ester linkage group, the result of the fit is shown in Figure 1 and appears to be reasonably close to the experimental phase diagram [17]. The dependence of the LCSTs of polyester series on m/n ratio shown in Figure 3 was calculated with the aforementioned values of parameters, varying only m and n. The calculated trend exhibits the same behavior as shown by the experimental data [17]. One can see that the curve levels off at large values of m/n, which corresponds to the polymer phase behavior being dominated by EO segments, asymptotically approaching the LCST value of pure PEO.

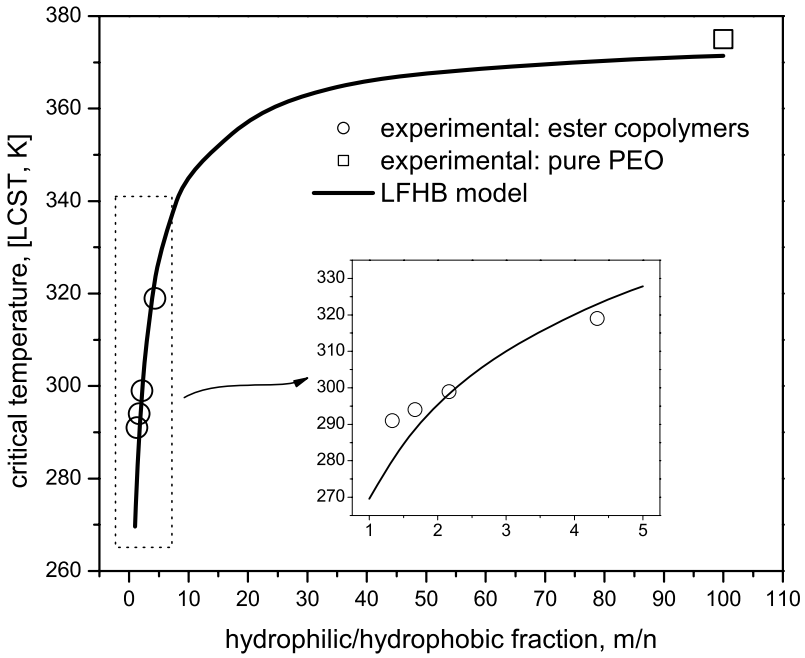

FIGURE 3. LCST dependence on hydrophilic/hydrophobic balance m/n for polyester series, calculated as described in section Polyester EO-EE copolymers

$$[—CH_2—(CH_2—O—CH_2)_m—CH_2—\underset{\underset{\|}{O}}{C}—\underset{\underset{|}{H}}{N}—(CH_2—CH_2)_n—\underset{\underset{|}{H}}{N}—\underset{\underset{\|}{O}}{C}—]_N \tag{51}$$

Similarly to the esters, when amide linkage groups (51) are introduced in the EO-EE copolymer, the N-H group brings in an additional type of donor, in addition to the ester C=O discussed above. Now, each P(EO-EE) molecule has ${d_2}^2 = 2 \cdot \mathrm{N}$ donors of the second type, equal to the number of N-H groups, ${a_2}^2 = m \cdot \mathrm{N}$ acceptors of the second type, equal to the number of EO segments, and ${a_3}^2 = 2 \cdot \mathrm{N}$ acceptors of the third type, equal to the number of C=O groups. Polymer–polymer hydrogen bond formation has a relatively small probability and can be ignored in the case of dilute solutions, thus we consider four types of H-bonds: $(1,1)$, $(1,2)$, $(1,3)$, $(2,1)$ - water–water, water–polymer(–O–), water–polymer(C=O), polymer(N–H)–water. As in the case of the polyester, this modification leaves the lattice-fluid part unchanged, but introduces two additional terms to the hydrogen bonding part of the chemical potential

$$\frac{\mu_{2,HB}}{k_B T} = r_2(\nu_{11}+\nu_{12}+\nu_{13}+\nu_{21}) + {d_2}^2 \ln\left(1-\frac{r\nu_{21}}{{d_2}^2 x_2}\right) + {a_2}^2 \ln\left(1-\frac{r\nu_{12}}{{a_2}^2 x_2}\right) + {a_3}^2 \ln\left(1-\frac{r\nu_{13}}{{a_3}^2 x_2}\right) \tag{52}$$

$$\frac{\mu_{1,HB}}{k_B T} = r_1(\nu_{11}+\nu_{12}+\nu_{13}+\nu_{21}) + {d_1}^1 \ln\left(1-\frac{r(\nu_{11}+\nu_{12}+\nu_{13})}{{d_1}^1 x_1}\right) + {a_1}^1 \ln\left(1-\frac{r(\nu_{11}+\nu_{21})}{{a_1}^1 x_1}\right) \tag{53}$$

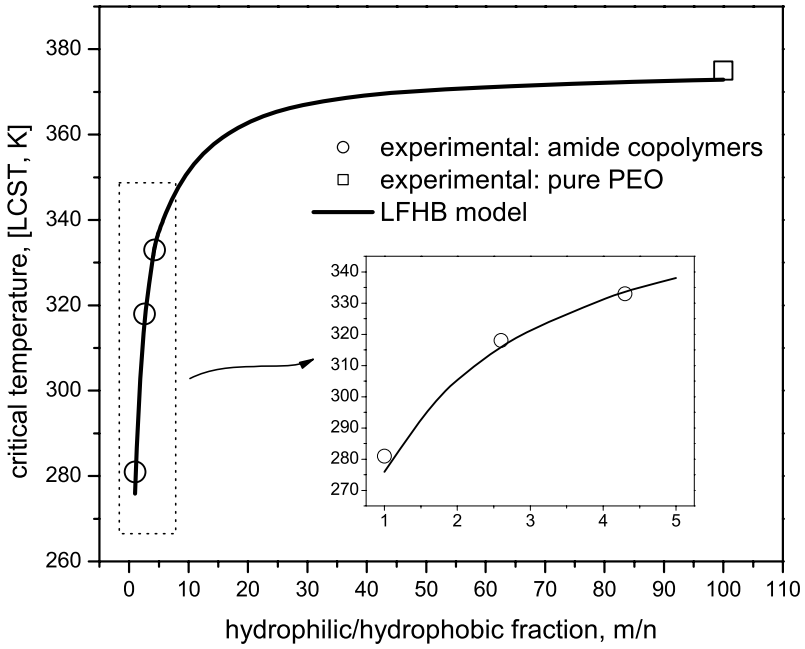

FIGURE 4. LCST dependence on hydrophilic/hydrophobic balance m/n for polyamide series, calculated as described in section Polyamide EO-EE copolymers

and results in two additional equations to the system of the equations of state, keeping the same form of the reduced density equation

$$\begin{cases} \mathscr{D}_1\mathscr{A}_1 - r\nu_{11}A_{11} = 0 \\ \mathscr{D}_1\mathscr{A}_2 - r\nu_{12}A_{12} = 0 \\ \mathscr{D}_1\mathscr{A}_3 - r\nu_{13}A_{13} = 0 \\ \mathscr{D}_2\mathscr{A}_1 - r\nu_{21}A_{21} = 0 \end{cases} \quad \text{where} \quad \begin{array}{l} \mathscr{D}_1 = {d_1}^1 x_1 - r(\nu_{11}+\nu_{12}+\nu_{13}) \\ \mathscr{D}_2 = {d_2}^2 x_1 - r\nu_{21} \\ \mathscr{A}_1 = {a_1}^1 x_1 - r\nu_{11} \\ \mathscr{A}_2 = {a_2}^2 x_2 - r\nu_{12} \\ \mathscr{A}_3 = {a_3}^2 x_2 - r\nu_{13} \end{array} \quad \begin{array}{l} A_{11} = r\tilde{v}\exp\left({G_{11}}^0/RT\right) \\ A_{12} = r\tilde{v}\exp\left({G_{12}}^0/RT\right) \\ A_{13} = r\tilde{v}\exp\left({G_{13}}^0/RT\right) \\ A_{21} = r\tilde{v}\exp\left({G_{21}}^0/RT\right) \end{array} \tag{54}$$

which brings the number of equations needed for finding the critical point to 17. In this manner, after the introduction of this additional hydrogen-bonding, the previous LFHB is used with the same values as for the esters and with no further fitting, i.e., with the parameter values from Table 1, and the same pair of ξ_{12}-parameters, which were obtained from the binodals of PEO and of the homologous polyester. The LCST vs. m/n curve calculated for the copolymers with the amide linkage group is shown in Figure 4 and exhibits excellent correlation with the experimental data [17]. This agreement is despite the fact that none of the parameters in the LFHB model were recalculated or adjusted for this system, which, to a certain extent, proves the consistency of the model and the validity of the assumption that the EO-EE copolymer phase behavior can be accounted through a "superposition" of the EO and EE aqueous phase behaviors.

Effect of Molecular Weight

To further test the validity of the model and of our assumptions, the influence of other parameters of the model was also investigated. In particular, we checked the dependence on polymer molecular weight, since the model has a complex explicit dependence on r, and consequently on the size of the polymer (i.e., the number of segments on

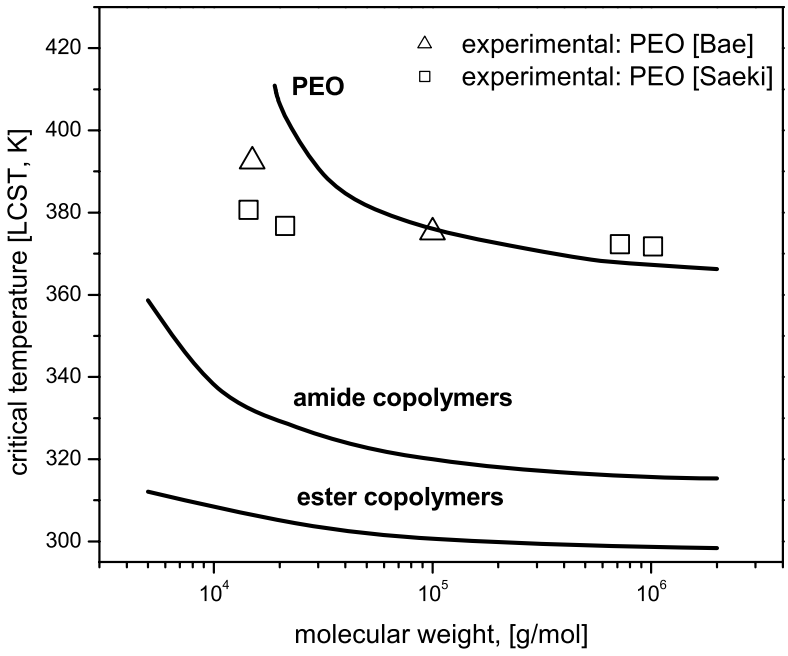

FIGURE 5. LCST dependence on molecular weight M_w for PEO, and EO-EE polyester and polyamide copolymers.

the quasi-lattice is dependent upon the polymer size). Focusing on PEO homopolymers, the calculated LCST values as a function of the M_w are plotted in Figure 5, and are compared with experimental values [29, 30] showing a decent qualitative agreement for the trend of polymer size on the PEO LCST. Specifically, the phase diagram of $M_w = 10^5$ PEO [29] was fitted with the calculated PEO binodal setting ${\xi_{12}}^{EO} = 1.0464$ (the fit of PEO coexisting curve for $M_w = 1.02 \cdot 10^6$ [30] returned a similar value ${\xi_{12}}^{EO} = 1.0467$). In addition, after obtaining the corresponding ${\xi_{12}}^{EE} = 1.0598$ as before, from the fit of $M_w = 5.75 \cdot 10^5, m = 13, n = 6$ polyester coexistence curve, the critical temperatures of the polyester copolymers were also calculated for the molecular weight values reported for each polymer [17](i.e., $M_w = 3.80 \cdot 10^5$ for $m = 13, n = 6$, $M_w = 2.45 \cdot 10^5$ for $m = 5, n = 3$, and $M_w = 3.00 \cdot 10^5$ for $m = 4, n = 3$). The calculated LCST values, shown in Figure 7, exhibit excellent agreement with the experimental data, compared to the previous case which disregarded the molecular weight dependence (*cf.* dotted line in Figure 7). Along the same lines, we also show in Figure 5 the molecular weight dependence of the EO-EE copolymers with ester and amide linkage groups. As expected [10], there is a weaker M_w dependence on the LCST for the copolymers compared to PEO, which is of importance for the design and synthesis of these systems, but which has not been systematically verified experimentally. Figure 6 shows the binodal curves calculated for the polyester series with the experimental values of molecular weights as described above. With the molecular weights in the given range one can see no significant difference in the shape of the binodal curves and in the values of critical concentration for the different sets of m, n values.

Finally, the experimental cloud point temperatures reported in [17] are in fact measured for $1wt\%$ polymer solutions and do not strictly correspond to the LCST values (although $\varphi_{poly} = 1wt\%$ lies in the near vicinity of the critical concentration for the reported molecular weights of the copolymers). Thus it makes some sense to compare those experimental data against the binodal temperatures at a weight fraction of polymer equal to 0.01 and for the experimentally reported M_w, rather than against against the LCST of a representative M_w (*cf.* Figure 3). This comparison is shown in Figure 7 for the ester copolymers, showing a very good agreement with the experimental data.

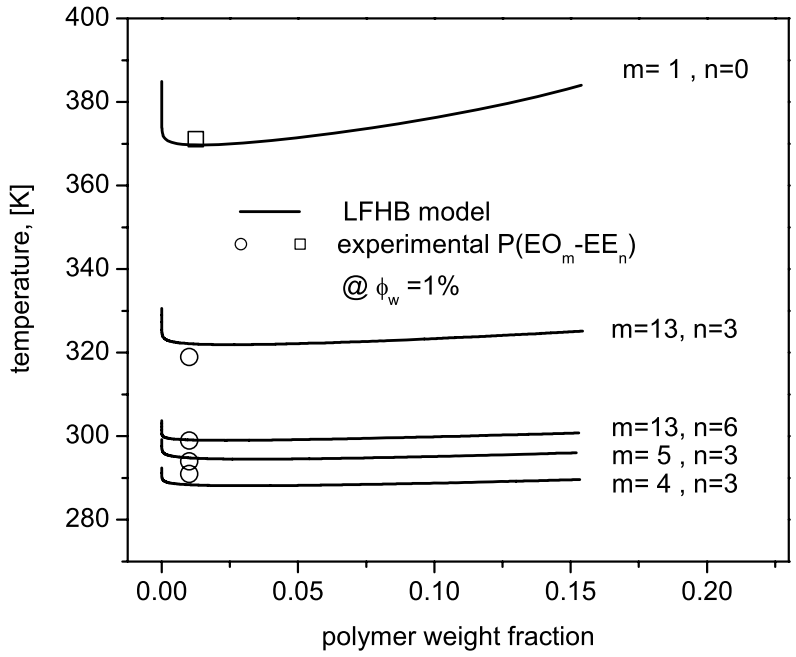

FIGURE 6. Binodals for polyester series calculated with experimental values of M_w as decribed the Effect of Molecular Weight section and experimental cloud point temperatures at $1wt\%$ polymer solution.

CONCLUDING REMARKS

The LFHB model in the form of the equations of state is suitable for describing the thermodynamic properties of polymer solutions over an extended range of external conditions. The model accounts for both water-polymer and water-water H-bond formation, overcoming the drawback of many alternative approaches, which ignore the water-water interaction. However, due to the purely statistical nature of the hydrogen-bonding part of the partition function, the relative orientation of donor and acceptor sites is not accounted for in the explicit form. In the lattice-fluid part the model retains mean-field approximate character and inherent shortcomings, making it impossible to take into account a number of important effects for the polymers in question, namely the difference between alternating, random, and especially highly-segmented or block copolymers, as well as the effects of end-groups.

Despite these drawbacks, the LFHB model, as applied in this study, captured the phase behavior for water solutions of PEO, and oligo(m)-EO and oligo(n)-EE ester and amide copolymers observed experimentally. In particular, it reproduced the critical temperatures dependence on the hydrophilic/hydrophobic balance for two series of copolymers, with the model parameters obtained from one PEO homopolymer and one polyester copolymer and used without further adjustment to the rest of the esters and to the amide series. This agreement leads to a few important, albeit rather qualitative, conclusions on the phase behavior of these uncharged copolymers: (a) the phase behavior of such systems is heavily controlled by the hydrogen-bonding, rather than the van der Waals or other interactions; (b) the LCST, and to some extent the binodal, can be predicted on the basis of the PEO aqueous phase behavior after simple weighted-addition of hydrophobic contributions, and thus can be related back to the hydrophilic/hydrophobic balance in the copolymer composition; and (c) suggests that the effects of the water network distortion by the introduction of hydrophobic groups, beyond the trivial reenumeration of hydrogen bonding probabilities, are probably small. On this last remark, one should consider that the parameter values, as obtained from the fitting of binodals of aqueous

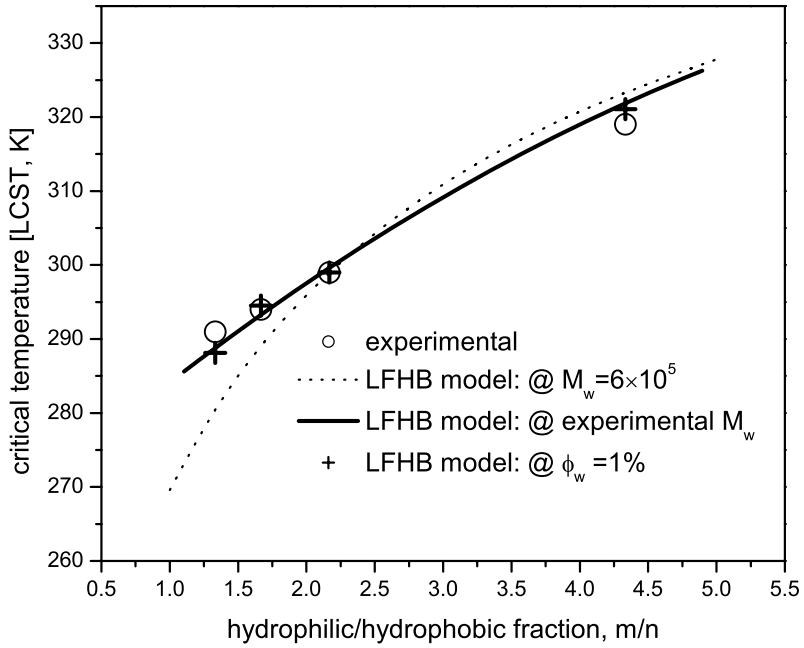

FIGURE 7. LCST as a function of hydrophilic/hydrophobic balance m/n for polyester series with explicit M_w dependence, i.e. calculated accounting for the experimental M_w of each system; the cross symbols show the coexistence temperature as a function of hydrophilic/hydrophobic balance m/n for the polyester copolymers, at a polymer weight fraction of 0.01 in solution and for the experimental M_w

solutions, do arguably include implicitly the energetics of the water (solvent). Thus a safer wording would be that the effects of the water network distortion for the (ethylene oxide)/ethylene copolymers are similar to the effects in poly(ethylene oxide) aqueous solutions.

Higher fidelity mean-field approaches, including modifications based on a quasi-chemical lattice-fluid framework [31, 32] and on hydrogen bonding cooperativity [18, 33], as well as molecular based simulations [34], are the focus of current work, so as to obtain more insights into the phase behavior –and ultimately into quantitative design principles– of polymers with tunable temperature response.

ACKNOWLEDGMENTS

This work was supported by the ONR (grant# 00014-05-1-0614) and the NSF (DMR-0602877, a MPS/Polymer and MWN award).

REFERENCES

1. H. Walter, D. E. Brooks, and D. Fisher, editors, *Partitioning in aqueous two-phase systems: theory, methods, uses, and applications to biotechnology*, Academic Press, 1985.
2. I. C. Sanchez, and R. H. Lacombe, *Macromolecules* **11**, 1145–1156 (1978).
3. C. G. Panayiotou, *Macromolecules* **20**, 861–871 (1987).
4. C. Panayiotou, and I. C. Sanchez, *Macromolecules* **24**, 6231–6237 (1991).
5. C. Panayiotou, and I. C. Sanchez, *J. Phys. Chem.* **95**, 10090–1097 (1991).
6. S. Bekiranov, R. Bruinsma, and P. Pincus, *Phys. Rev. E* **55**, 577–585 (1997).
7. E. E. Dormidontova, *Macromolecules* **35**, 987–1001 (2002).
8. D. C. Kannan, J. L. Duda, and R. P. Danner, *Fluid Phase Equilibria* **237**, 86–88 (2005).
9. L. D. Taylor, and L. D. Cerankowski, *J. Polym. Sci., Polym. Chem Ed.* **13**, 2551–2570 (1975).
10. E. Manias, M. Rackaitis, and K. E. Strawhecker, *US Patent* **7,011,930** (2006).
11. G. Bokias, D. Hourdet, and I. Iliopoulos, *Macromolecules* **33**, 2929–2935 (2000).
12. J. Virtanen, S. Holappa, H. Lemmetyinen, and H. Tenhu, *Macromolecules* **35**, 4763–4769 (2002).
13. A. N. Rissanou, S. H. Anastasiadis, and I. A. Bitsanis, *J. Polym. Sci. B: Polym. Phys.* **44**, 3651–3666 (2006).
14. S. Furyk, Y. Zhang, D. Ortiz-Acosta, P. S. Cremer, and D. E. Bergbreiter, *J. Polym. Sci. A* **44**, 1492–1501 (2006).
15. Y. Nagasaki, F. Matsukura, M. Kato, H. Aoki, and T. Tokuda, *Macromolecules* **29**, 5859–5863 (1996).
16. H. O. Johansson, M. Svensson, J. Persson, and F. Tjerneld, "Aqueous two-phase systems with smart polymers," in *Smart Polymers for Bioseparation and Bioprocessing*, edited by I. Y. Galaev, and B. Mattiasson, 2004.
17. M. Rackaitis, K. Strawhecker, and E. Manias, *J. Polym. Sci. B: Polym. Phys.* **40**, 2339–2342 (2002).
18. C. G. Panayiotou, "Hydrogen Bonding in Solutions: The Equation-of-State Approach," in *The Handbook of Surface and Colloid Chemistry*, edited by K. S. Birdi, 2003.
19. J. M. Prausnitz, R. N. Lichtenthaler, and E. Gomes de Azavedo, *Molecular Thermodynamics of Fluid-Phase Equilibria*, Prentice Hall, 1999.
20. B. A. Veytsman, *J. Phys. Chem.* **94**, 8499–8500 (1990).
21. S. Levine, and J. W. Perram, "A Statistical Mechanical Treatment of Hydrogen-Bonding in Water," in *Hydrogen-Bonded Solvent Systems*, edited by A. K. Covington, and P. Jones, 1968.
22. E. Manias, V. Kuppa, D. K. Yang, and D. B. Zax, *Colloids Surf., A* **187**, 509–521 (2001).
23. V. Kuppa, S. Menakanit, R. Krishnamoorti, and E. Manias, *J. Polym. Sci. B: Polym. Phys.* **41**, 3285–3298 (2003).
24. V. Kuppa, and E. Manias, *J. Chem. Phys.* **118**, 3421–3429 (2003).
25. I. C. Sanchez, and C. Panayiotou, "Equation of State Thermodynamica of Polymer and Related Solutions," in *Models of Thermodynamic and Phase Equilibria Calculations*, edited by S. Sandler, 1994.
26. M. J. D. Powell, "A Fortran Subroutine for Solving Systems of Nonlinear Algebraic Equations," in *Numerical Methods for Nonlinear Algebraic Equations*, edited by P. Rabinowitz, 1970.
27. R. B. Gupta, C. G. Panayiotou, I. C. Sanchez, and K. P. Johnston, *AIChE J.* **38**, 1243–1253 (1992).
28. A. K. Lele, M. V. Badiger, M. M. Hirve, and R. A. Mashelkar, *Chem. Eng. Sci.* **50**, 3535–3545 (1995).
29. Y. C. Bae, J. J. Shim, D. S. Soane, and J. Prausnitz, *J. Appl. Polym. Sci.* **47**, 1193–1206 (1993).
30. S. Saeki, N. Kuwahara, M. Nakata, and M. Kaneko, *Polymer* **17**, 685–689 (1976).
31. M. Taimoori, and C. Panayiotou, *Fluid Phase Equilibria* **192**, 155–169 (2001).
32. T. Vlachou, I. Prinos, J. H. Vera, and C. G. Panayiotou, *Ind. Eng. Chem. Res.* **41**, 1057–1063 (2002).
33. D. Missopolinou, and C. Panayiotou, *J. Phys. Chem. A* **102**, 3574–3581 (1998).
34. E. A. Tritopoulou, and I. G. Economou, *Fluid Phase Equilibria* **248**, 134–146 (2006).